Interaction of Ph_2Zn with 1,3-Xylyl Crown Ethers. Crystal Structures of Three 1:1 Complexes

Peter R. Markies, Gerrit Schat, Otto S. Akkerman, and Friedrich Bickelhaupt*

Scheikundig Laboratorium, Vrije Universiteit, De Boelelaan 1083, NL-1081 HV Amsterdam, The Netherlands

Wilberth J. J. Smeets and Anthony L. Spek

Vakgroep Kristal- en Structuurchemie, University of Utrecht,
Padualaan 8, NL-3584 CH Utrecht, The Netherlands

Received March 19, 1991

The behavior of diphenylzinc toward four 1,3-xylyl crown ethers was investigated. Only "simple" complexation occurred, whereas diphenylmagnesium had previously been shown to lead to halogen–metal exchange, metalation, or rotaxane formation. Three of the 1:1 complexes were obtained as crystalline solids and characterized by X-ray crystal structure determination; 1,3-xylyl 15-crown-4 (1) gave an oily adduct. Crystals of diphenylzinc–2-bromo-1,3-xylyl 15-crown-4 (8) are monoclinic, space group $P2_1/n$, with unit cell dimensions a = 9.800 (1) Å, b = 12.887 (1) Å, c = 19.671 (2) Å, β = 95.66 (1)°, and Z = 4. Crystals of diphenylzinc–2-bromo-1,3-xylyl 18-crown-5 (9) are monoclinic, space group $P2_1/n$, with unit cell dimensions a = 9.368 (1) Å, b = 10.975 (1) Å, c = 27.051 (2) Å, β = 97.48 (2)°, and Z = 4. Crystals of diphenylzinc–1,3-xylyl 18-crown-5 (10) are monoclinic, space group $P2_1/n$, with unit cell dimensions a = 14.775 (3) Å, b = 18.252 (3) Å, c = 20.082 (1) Å, β = 103.29 (1)°, and Z = 8; two independent but chemically equivalent residues are present in the unit cell. The three molecular structures are closely related: the zinc atom is tetrahedrally surrounded by two phenyl groups and by two of the oxygens of the crown ether. These organozinc complexes may serve as (stable!) models for intermediate stages in the above-mentioned reactions of organomagnesium compounds with crown ethers.

Introduction

We have reported[1-3] reactions between certain 1,3-xylyl crown ethers and diphenylmagnesium or phenylmagnesium bromide (Schemes I and II). With 1,3-xylyl 15-crown-4 (1), a remarkable metalation reaction occurred. 2-Bromo-1,3-xylyl 15-crown-4 (2) and 2-bromo-1,3-xylyl 18-crown-5 (3) underwent halogen–metal exchange reactions. Such reactivity is well-known in organolithium chemistry but quite unusual for organomagnesium compounds. Therefore, a specific, activating complexation between the crown ether and the organomagnesium reagent was proposed to play a decisive role in inducing these reactions.

The metalation reaction shows a high substrate selectivity: it did occur with 1 but not with the higher homologue 1,3-xylyl 18-crown-5 (4), which yielded a 1:1 complex instead. Its X-ray crystal structure revealed an interesting rotaxane structure 7,[2] with a nearly linear Ph–Mg–Ph unit threading the crown ether cavity (Scheme II). In toluene solution, 7 is in equilibrium with an isomer 5, which probably has a "side-on" structure. Interconversion of these complexes was postulated to proceed under the influence of a second molecule of diphenylmagnesium: dissociation of one of the C–Mg bonds furnishes intermediate 6, which contains a magnesate unit.[4,5]

Scheme I

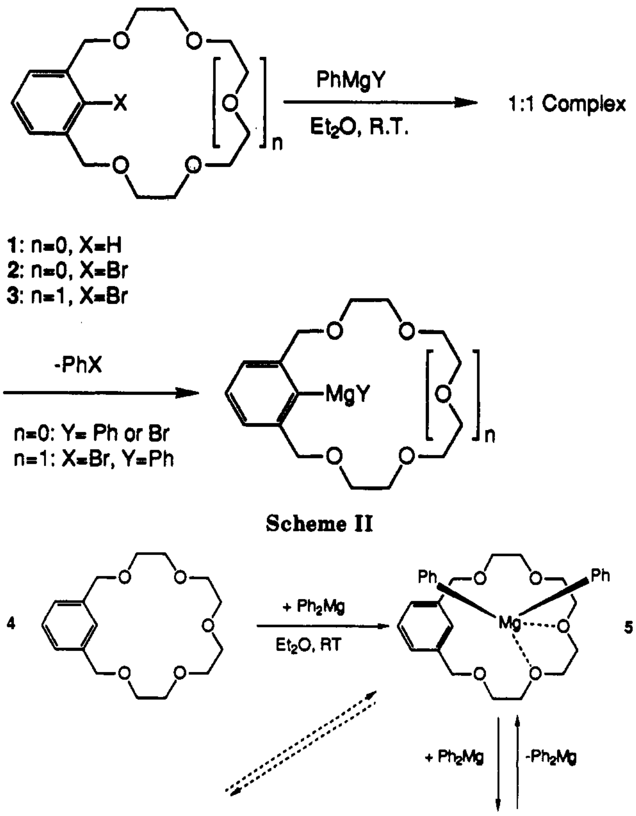

Scheme II

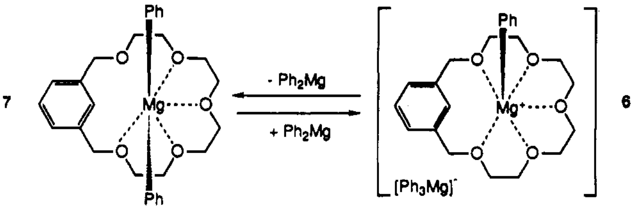

In view of these unexpected reactions of phenylmagnesium compounds with crown ethers, it was of interest to investigate the behavior of other metals. An obvious choice was zinc, an element whose organometallic chemistry shows many analogies with that of magnesium. Therefore, the reaction between diphenylzinc and the four crown ethers 1–4 was studied. A priori, metalation or halogen–metal exchange reactions were less likely, because

---

(1) Markies, P. R.; Nomoto, T.; Akkerman, O. S.; Bickelhaupt, F.; Smeets, W. J. J.; Spek, A. L. *Angew. Chem.* 1988, *100*, 1143.

(2) Markies, P. R.; Nomoto, T.; Akkerman, O. S.; Bickelhaupt, F.; Smeets, W. J. J.; Spek, A. L. *J. Am. Chem. Soc.* 1988, *110*, 4845.

(3) Smeets, W. J. J.; Spek, A. L.; Markies, P. R.; Nomoto, T.; Akkerman, O. S.; Bickelhaupt, F. *Z. Kristallogr.* 1988, *185*, 371.

(4) Squiller, E. P.; Whittle, R. R.; Richey, H. G., Jr. *J. Am. Chem. Soc.* 1985, *107*, 432.

(5) Squiller, E. P.; Whittle, R. R.; Richey, H. G., Jr. *Organometallics* 1985, *4*, 1154.

0276-7333/91/2310-3538$02.50/0

zinc is less electropositive than magnesium (X = 1.65 and 1.31, respectively[6]), but it was conceivable that the crown ether activation would be sufficient to facilitate such reactivity, even for an inherently less reactive organozinc reagent.

On the other hand, if stable complexes were formed, their characterization by an X-ray crystal structure determination was expected to be of interest for several reasons:

(1) Our understanding of the remarkable organomagnesium reactions might be improved by identification of zinc analogues of nonisolable intermediates such as **5**.

(2) In analogy to **7**, a crown ether–diphenylzinc rotaxane might be formed. In this context, the rotaxane structures of diethylzinc,[7a] diethylmagnesium,[7a] and the dimethylaluminum cation[7b] with crown ethers should be mentioned.

(3) Structural data of arylzinc compounds were practically nonexistent. In fact, our recent study of solvent-free diphenylzinc, which was found to be a dimer, presents so far the only X-ray crystallographic characterization of an arylzinc compound.[8]

(4) Since the beginning of organozinc chemistry, it is known that simple dialkyl- or diarylzinc compounds form intermolecular, weak complexes with ethers,[9] but structural data are scarce; they are important for understanding the physical behavior and reactions of these compounds.

(5) Structural data of organozinc reagents may be useful for parametrization purposes in semiempirical calculations for this type of organometallic compounds.[10,11]

Results and Discussion

The reactions between diphenylzinc and the 1,3-xylyl crown ethers **1**–**4** were performed by mixing the components in a 1:1 stoichiometry in diethyl ether. From the resulting clear solution, the crystalline products $Ph_2Zn \cdot \mathbf{2}$ (**8**), $Ph_2Zn \cdot \mathbf{3}$ (**9**), and $Ph_2Zn \cdot \mathbf{4}$ (**10**) were obtained by slowly concentrating and cooling; crown ether **1** yielded a colorless oil containing only a trace of solid material, even upon complete removal of the solvent and subsequent cooling. Crystalline **8**–**10** were separated from the mother liquor by decantation and dried. An aliquot of the crystals was pumped under high vacuum to remove the last traces of solvent and dissolved in a deuterated solvent (toluene-d_8 or C_6D_6) for characterization by ^1H NMR spectroscopy, which indicated the formation of stable, solvent free 1:1 complexes **8**–**10** (see under Experimental Section). The NMR spectra were straightforward and did not reveal dynamic processes or chemical transformations. Reference spectra of the pure crown ethers under identical conditions showed that, upon complexation, the crown ether signals were generally shielded by 0.1–0.2 ppm, and the coupling patterns of the C_2H_4 units and benzylic CH_2 groups (AA′BB′ and AB multiplets, respectively) were broadened due to the diminished flexibility of the crown ether.

Thus, diphenylzinc was unreactive under conditions where the organomagnesiums induced the crown ethers to undergo metalation or halogen–metal exchange (Scheme I) or rotaxane formation (Scheme II).

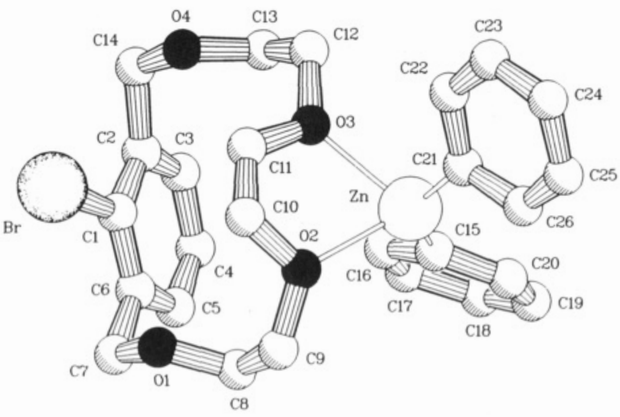

Figure 1. PLUTON drawing for complex **8**. The hydrogen atoms are omitted for clarity.

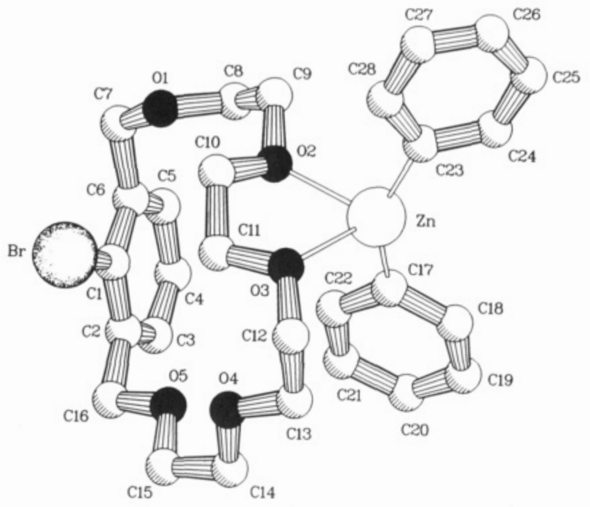

Figure 2. PLUTON drawing for complex **9**. The hydrogen atoms are omitted for clarity.

In an attempt to enforce a reaction, the experiments were repeated in toluene at an elevated temperature (100 °C, 6 h). The reaction mixtures were quenched with H_2O or D_2O to analyze changes at the aryl 2-positions (replacement of the original Br or H substituent by H or D). In none of the cases was any indication of halogen or hydrogen exchange detected; the crown ethers **1**–**4** were recovered unchanged and in high yield. Obviously, the activating power of the crown ether moieties is sufficient to coax organomagnesium, but not organozinc compounds, into mimicking organolithium-like behavior.

The crystalline complexes **8**–**10** were stable and did not deteriorate under vacuum. Their solid-state structures were elucidated by X-ray crystal structure determinations. Three similar structures were found (Figures 1–3), in which the diphenylzinc unit is coordinating in a side-on fashion to two neighboring oxygen atoms of the crown ether ring. The coordination of the metal does not involve one of the benzylic oxygens; probably, minimization of steric hindrance is responsible, but a slightly lower basicity of the benzylic ether function due to the inductive effect of the benzene ring may also play a role. The zinc atom is surrounded in a pseudotetrahedral fashion by two phenyl groups and two of the crown ether oxygens, with small O–Zn–O and large C–Zn–C angles (vide infra).

The formation of the side-on complexes in all cases probably indicates that, under these conditions, diphenylzinc reaches its coordinative saturation on tetracoordination. In this context, the coordinative behavior of trialkylaluminum compounds with crown ethers may

---

(6) Allred, A. L. *J. Inorg. Nucl. Chem.* **1961**, *17*, 215.

(7) (a) Pajerski, A. D.; Parvez, M.; Richey, H. G., Jr. *J. Am. Chem. Soc.* **1988**, *110*, 4844. (b) Bott, S. G.; Alvanipour, A.; Money, S. D.; Atwood, D. A.; Means, C. M.; Coleman, A. W.; Atwood, J. L. *Angew. Chem.* **1987**, *99*, 476.

(8) Markies, P. R.; Akkerman, O. S.; Bickelhaupt, F.; Smeets, W. J. J.; Spek, A. L. *Organometallics* **1990**, *9*, 2243.

(9) Boersma, J. In *Comprehensive Organometallic Chemistry*; Wilkinson, G., Ed.; Pergamon: Oxford, **1982**; Vol. 2, p 823.

(10) Dewar, M. J. S.; Merz, Jr., K. M. *Organometallics* **1986**, *5*, 1494.

(11) Dewar, M. J. S.; Merz, Jr., K. M. *Organometallics* **1988**, *7*, 522.

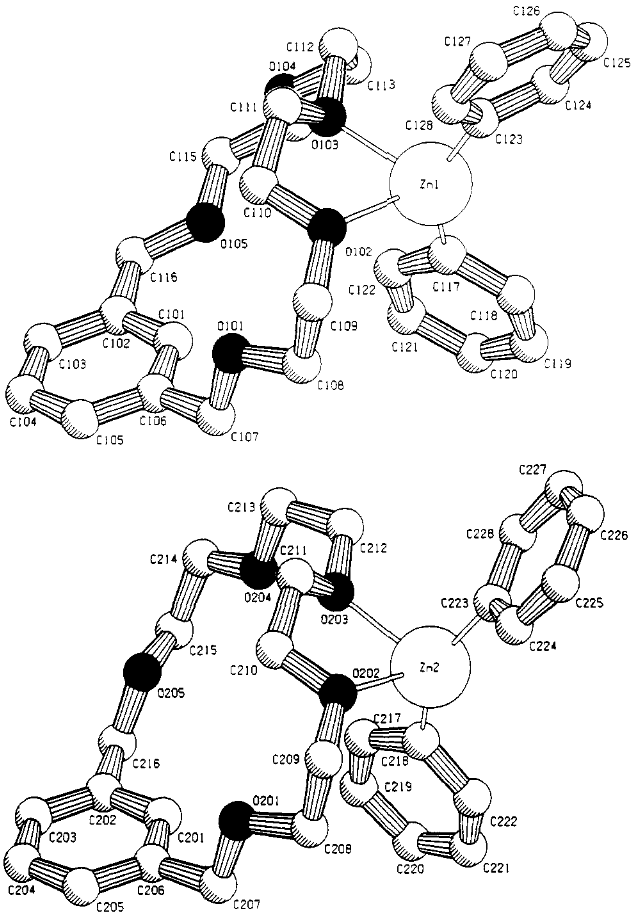

Figure 3. PLUTON drawings for complexes **10a,b**. The hydrogen atoms are omitted for clarity.

be relevant. Bonded to three alkyl groups, the metal atom needs only one coordinative bond to an ether molecule to complete a (pseudo)tetrahedral coordination. In this way, a single crown ether molecule can bind one or several trialkylaluminums in a monohapto fashion, as illustrated by the crystal structures of dibenzo-18-crown-6·$(Me_3Al)_3$, 18-crown-6·$(Me_3Al)_4$,[12] 12-crown-4·$(Me_3Al)_2$,[13] dicyclohexano-18-crown-6·$(Me_3Al)_2$,[14] and 1,4,8,11-tetrathiacyclotetradecane·$(Me_3Al)_4$.[15] Structures in which a trialkylaluminum moiety resides *inside* the cavity of a crown ether are not known. Other relevant examples of side-on complexes are the adducts 18-crown-6·MCl_4 (M = Ti or Sn),[16] in which the crown ether acts as a bidentate ligand toward a pseudooctahedrally surrounded metal atom.

In spite of an overall similarity between the three crystal structures **8**–**10**, it is important to discuss the specific differences due to ring size and the substituent at the xylyl 2-position. In all three cases, the crown ether acts as a bidentate ligand, but possibly for different reasons. In the 2-bromo xylyl crown ethers **2** and **3**, there is practically no space available in the cavity because of the large intraannular bromine substituent; thus, the formation of "rotaxane" complexes is prevented. Moreover, the crown ethers have a limited conformational flexibility. These effects are most pronounced in **2**, which also suffers from steric strain (intramolecular van der Waals contacts; it was not possible to construct a CPK model of **2**), and the ^1H NMR spectrum of **2** revealed an AB system for the benzylic CH_2 group and complicated C_2H_4 multiplets, indicative of the restricted conformational mobility. A recently published crystal structure of **3** revealed an interesting phenomenon: its conformation is quite similar to that of **9**; in a sort of "self-complexation", one of the ethylene units is turned inward into the crown ether cavity.[17] While a crystal structure of **2** is not available, its complex **8** shows several intramolecular, short, nonbonded contacts (Br–C(10) 3.97 (1) Å, Br–C(11) 3.75 (1) Å, Br–O(1) 3.322 (5) Å, Br–O(4) 3.344 (5) Å). Crown ethers **2** and **3** may in fact be considered as effective bidentate ligands that are sterically preorganized in such a way that two oxygen atoms are readily accessible for external coordination.

With **4**, the situation is quite different. This ligand does not have a bulky substituent at the xylyl 2-position blocking the cavity; from the crystal structure,[18] it is evident that a (small) cavity is indeed available. Furthermore, **4** has more conformational flexibility than **1**–**3**. This can be deduced from its crystal structure, the study of models, and the crystal structure of its complexes with diphenylmagnesium[2] and with *tert*-butylammonium perchlorate,[19] in which the ligand adopts conformations that are different from that of free **4**.[18] Therefore, a diphenylzinc rotaxane structure analogous to that of **7** seemed feasible. Why then does it not occur?

We feel that three factors may play a role. In the first place, the Lewis acidity of diphenylzinc is weaker than that of diphenylmagnesium, so, in general, the zinc compound forms weaker complexes; indeed, organozinc compounds usually exhibit a tetrahedral coordination geometry.[9] Diphenylzinc will certainly have a less pronounced demand than diphenylmagnesium to attain the high coordination number of six, which goes along with rotaxane formation (cf. **7**, Scheme II). However, this factor alone cannot be decisive, as a rotaxane complex between diethylzinc and 18-crown-6 is known[7a] (which, admittedly, has less steric hindrance inside its cavity!). We therefore suggest that diphenylzinc and **4** do not form a rotaxane complex, because this process is not possible for *kinetic* reasons: two obvious modes of its formation are blocked. Direct insertion of diphenylzinc into the cavity of **4** is not possible because the cavity is too small to allow the passage of a phenyl group; this was already pointed out for the corresponding reaction of diphenylmagnesium and **4**.[2,18] The alternative mode of formation parallels that depicted for diphenylmagnesium in Scheme II; it would require dissociation of a phenyl anion from diphenylzinc under formation of a (solvated) phenylzinc cation and a triphenylzincate anion, in analogy to the transformation **5** → **6**. Apparently, this step is not possible because the polarity of the zinc–phenyl bond is insufficient and, possibly, because diphenylzinc is a weaker Lewis acid than diphenylmagnesium. Thus, a low-energy pathway for rotaxane formation not being available, the complex formation stops at the level of the primary side-on complex **10**. In this context, it should be pointed out that according to the ^1H NMR spectra, solutions of **10** in toluene-d_8 were unchanged after several weeks; under the same conditions,

---

(12) Atwood, J. L.; Priester, R. D.; Rogers, R. D.; Canada, L. G. *J. Inclusion Phenom.* **1983**, *1*, 61.

(13) Robinson, G. H.; Bott, S. G.; Elgamal, H.; Hunter, W. E.; Atwood, J. L. *J. Inclusion Phenom.* **1985**, *3*, 65.

(14) Robinson, G. H.; Hunter, W. E.; Bott, S. G.; Atwood, J. L. *J. Organomet. Chem.* **1987**, *326*, 9.

(15) Robinson, G. H.; Zhang, H.; Atwood, J. L. *Organometallics* **1987**, *6*, 887.

(16) Bott, S. G.; Prinz, H.; Alvanipour, A.; Atwood, J. L. *J. Coord. Chem.* **1987**, *16*, 303.

(17) Skowronska-Ptasinska, M.; Aarts, V. M. L. J.; Egberink, R. J. M.; van Eerden, J.; Harkema, S.; Reinhoudt, D. N. *J. Org. Chem.* **1988**, *53*, 5484.

(18) Smeets, W. J. J.; Spek, A. L.; Markies, P. R.; Nomoto, T.; Akkerman, O. S.; Bickelhaupt, F. *Acta Crystallogr.* **1989**, *C45*, 443.

(19) van Eerden, J.; Harkema, S.; Sudhölter, E. J. R. *Acta Crystallogr. C* **1986**, *42*, 201.

Table I. Crystal Data and Details of the Structure Determination of 8–10

		Crystal Data	
formula	$C_{26}H_{29}O_4ZnBr$	$C_{28}H_{33}O_5ZnBr$	$C_{28}H_{34}O_5Zn$
mol wt	550.80	594.85	515.95
cryst system	monoclinic	monoclinic	monoclinic
space group	$P2_1/n$(No. 14)	$P2_1/n$(No. 14)	$P2_1/n$(No. 14)
a, *b*, *c*, Å	9.800 (1), 12.887 (1), 19.671 (2)	9.368 (1), 10.975 (1), 27.051 (2)	14.775 (3), 18.252 (3), 20.082 (1)
β	95.66 (1)	97.48 (2)	103.29 (1)
V, Å^3	2472.2 (4)	2757.5 (5)	5271 (1)
Z	4	4	8
D_{calc}, g cm^{-3}	1.480	1.433	1.300
F(000)	1128	1224	2176
μ, (cm^{-1})	26.4	23.8	9.9
cryst size, mm	0.20 × 0.23 × 0.50	0.22 × 0.60 × 0.75	0.38 × 0.50 × 0.82
		Data Collection	
temp, K	295	295	295
θ_{min}, θ_{max}, deg	1.0, 27.5	0.76, 27.5	1.0, 24.0
radiatn	Mo Kα (Zr filtered), 0.71073 Å	Mo Kα (Zr filtered), 0.71073 Å	Mo Kα (Zr filtered), 0.71073 Å
$\Delta\omega$, deg	$0.55 + 0.35 \tan\theta$	$0.55 + 0.35 \tan\theta$	$0.60 + 0.35 \tan\theta$
hor and vert aperture, mm	3.0, 6.0	3.0, 6.0	3.0, 4.0
X-ray exposure time, h	91	99	123
linear decay, %	25	10.2	3.0
ref rflns	3,2,–6; 0,5,4	2,4,5;2,-4,5	4,-1,-4;3,-3,4
data set	*h*,0,12; *k*,0,16; *l*,-25,25	*h*,-12,12; *k*,0,14; *l*,0,35	*h*,0,16; *k*,-20,0; *l*,22,22
total data	6274	6786	8921
total unique data	5672	6311	8244
obsd data	2036 [$I > 2.5\sigma(I)$]	3226 [$I > 2.5\sigma(I)$]	4502 [$I > 2.5\sigma(I)$]
DIFABS correctn range	-	0.72–1.30	
		Refinement	
no. of rflns	2036	3226	4502
no. of refined params	290	318	615
weighting scheme	$w = 1.0/[\sigma^2(F) + 0.000429F^2]$	$w = 1.0/\sigma^2(F)$	$w = 1.0/\sigma^2(F)$
final, *R*, R_w, *S*	0.051, 0.050, 1.83	0.042, 0.043, 1.37	0.045, 0.032, 1.48
isotr therm param H atoms, Å^2	0.105 (6)	0.072 (2)	0.094 (2), 0.101 (3)
$(\Delta/\sigma)_{av}$ in final cycle	0.003	0.0003	0.05
min, max, resd dens, e/Å^3	-0.54, 0.44	-0.30, 0.49	-0.30, 0.29

5 and **7** are clearly discernible in equilibrium when **7** is dissolved in toluene-d_8.[2]

The asymmetric unit of the crystal structure of **10** contains two crystallographically independent molecules (**10a** and **10b**). The conformations of the two crown ether rings differ significantly in six ring torsion angles. This again illustrates the conformational freedom of **4**. In Table VIII, the diphenylzinc coordination geometries are listed for the three complexes. They present basically the same pattern, with some slight differences. The (covalent) Zn–C bonds are rather constant (1.947 (4)–1.973 (4) Å); the Zn–O coordination shows slightly more variation (2.228 (3)–2.393 (3) Å). Characteristic for all structures is the large C–Zn–C angle (139.6 (3)–149.9 (2)°). This value reflects the original sp hybridization of the zinc toward carbon, which is only partially disturbed by the coordinating ether oxygens; compared with a typical diphenylmagnesium complex ($Ph_2Mg{\cdot}2THF$:[20] C–Mg–C 122.4 (1)°), there is a clear tendency for more linearity of the C–Zn–C bond. The other angles around zinc are considerably smaller. The O–Zn–O angles, which are part of a five-membered ring, are between 72.6 (4) and 73.4 (1)°, and the C–Zn–O angles are between 96.8 (1) and 108.1 (1)°.

Our new diphenylzinc complexes are not only unique in being the first of their kind but also in importance by throwing light on our earlier results with diphenylmagnesium. This has already been discussed for the rotaxane formation but holds for the remarkable metalation and halogen–metal exchange reactions, too. These reactions were rationalized as occurring via the formation of an unstable initial complex that cannot be isolated (vide supra). Instead, the diphenylzinc complexes **8–10** may serve as stable models. This is illustrated for the combination of the reagents diphenylmagnesium and **2** (the

Table II. Final Coordinates and Equivalent Isotropic Thermal Parameters and Their Esd's in Parentheses for 8

atom	*x*	*y*	*z*	*U*(eq),[a] Å^2
Br	0.19301 (9)	0.16808 (7)	0.06500 (4)	0.0724 (4)
Zn	0.46450 (9)	0.30213 (8)	-0.19855 (4)	0.0719 (4)
O(1)	0.3286 (5)	0.0170 (4)	-0.0475 (2)	0.071 (2)
O(2)	0.5022 (6)	0.1819 (5)	-0.1142 (3)	0.080 (3)
O(3)	0.3745 (5)	0.3621 (5)	-0.1044 (3)	0.076 (3)
O(4)	0.1405 (6)	0.3938 (4)	-0.0173 (3)	0.078 (3)
C(1)	0.0837 (7)	0.1581 (7)	-0.0211 (3)	0.058 (3)
C(2)	-0.0010 (9)	0.2412 (7)	-0.0412 (4)	0.066 (3)
C(3)	-0.0897 (9)	0.2278 (9)	-0.0990 (5)	0.085 (5)
C(4)	-0.094 (1)	0.138 (1)	-0.1357 (5)	0.091 (5)
C(5)	-0.0026 (9)	0.0599 (8)	-0.1170 (4)	0.079 (4)
C(6)	0.0894 (8)	0.0685 (7)	-0.0590 (4)	0.059 (3)
C(7)	0.1918 (8)	-0.0165 (6)	-0.0397 (4)	0.073 (4)
C(8)	0.3613 (9)	0.0234 (7)	-0.1165 (4)	0.085 (4)
C(9)	0.5012 (9)	0.0723 (8)	-0.1183 (4)	0.087 (4)
C(10)	0.495 (1)	0.2244 (9)	-0.0508 (5)	0.119 (6)
C(11)	0.421 (1)	0.309 (1)	-0.0466 (5)	0.183 (8)
C(12)	0.292 (1)	0.4513 (7)	-0.0979 (4)	0.090 (4)
C(13)	0.1467 (9)	0.4271 (7)	-0.0866 (5)	0.083 (4)
C(14)	0.014 (1)	0.3462 (8)	-0.0073 (4)	0.087 (4)
C(15)	0.3133 (8)	0.2524 (6)	-0.2631 (4)	0.061 (3)
C(16)	0.1827 (9)	0.2290 (7)	-0.2447 (4)	0.073 (3)
C(17)	0.0740 (9)	0.2033 (7)	-0.2922 (4)	0.085 (4)
C(18)	0.094 (1)	0.2049 (7)	-0.3606 (4)	0.080 (4)
C(19)	0.223 (1)	0.2262 (7)	-0.3806 (4)	0.078 (4)
C(20)	0.3282 (9)	0.2491 (6)	-0.3323 (4)	0.068 (3)
C(21)	0.6317 (8)	0.3856 (7)	-0.1979 (4)	0.065 (3)
C(22)	0.6572 (9)	0.4731 (8)	-0.1589 (5)	0.084 (4)
C(23)	0.768 (1)	0.5361 (8)	-0.1622 (5)	0.089 (4)
C(24)	0.863 (1)	0.5136 (9)	-0.2053 (5)	0.092 (5)
C(25)	0.846 (1)	0.426 (1)	-0.2449 (5)	0.094 (5)
C(26)	0.731 (1)	0.3642 (8)	-0.2419 (4)	0.080 (4)

[a] U_{eq} = one-third of the trace of the orthogonalized **U** matrix.

---

[20] Markies, P. R.; Schat, G.; Akkerman, O. S.; Bickelhaupt, F.; Smeets, W. J. J.; Spek, A. L. *J. Organomet. Chem.* **1990**, *393*, 315.

Table III. Final Coordinates and Equivalent Isotropic Thermal Parameters and Their Esd's in Parentheses for 9

atom	*x*	*y*	*z*	*U*(eq),[a] Å^2
Br	0.09930 (6)	0.05936 (5)	0.11724 (2)	0.0697 (2)
Zn	0.04041 (5)	0.60452 (5)	0.15198 (2)	0.0532 (2)
O(1)	-0.1579 (3)	0.2282 (3)	0.0584 (1)	0.066 (1)
O(2)	-0.0674 (3)	0.4307 (3)	0.1246 (1)	0.053 (1)
O(3)	0.0972 (3)	0.4578 (3)	0.2136 (1)	0.054 (1)
O(4)	0.3843 (3)	0.3396 (3)	0.2160 (1)	0.062 (1)
O(5)	0.4182 (3)	0.2150 (3)	0.1263 (1)	0.067 (1)
C(1)	0.1546 (5)	0.1217 (4)	0.0565 (2)	0.054 (2)
C(2)	0.2995 (5)	0.1313 (4)	0.0526 (2)	0.057 (2)
C(3)	0.3369 (6)	0.1710 (4)	0.0071 (2)	0.072 (2)
C(4)	0.2344 (6)	0.2008 (5)	-0.0313 (2)	0.078 (2)
C(5)	0.0920 (6)	0.1937 (4)	-0.0259 (2)	0.068 (2)
C(6)	0.0472 (5)	0.1540 (4)	0.0185 (2)	0.057 (2)
C(7)	-0.1115 (5)	0.1454 (4)	0.0236 (2)	0.069 (2)
C(8)	-0.1553 (6)	0.3512 (4)	0.0431 (2)	0.075 (2)
C(9)	-0.1851 (5)	0.4303 (4)	0.0857 (2)	0.071 (2)
C(10)	-0.0759 (4)	0.3408 (4)	0.1625 (2)	0.054 (2)
C(11)	0.0698 (4)	0.3384 (4)	0.1936 (2)	0.053 (2)
C(12)	0.2193 (5)	0.4662 (5)	0.2515 (2)	0.069 (2)
C(13)	0.3617 (5)	0.4583 (5)	0.2331 (2)	0.065 (2)
C(14)	0.5165 (4)	0.3285 (4)	0.1958 (2)	0.060 (2)
C(15)	0.5191 (4)	0.2102 (4)	0.1696 (2)	0.060 (2)
C(16)	0.4158 (5)	0.1102 (4)	0.0957 (2)	0.069 (2)
C(17)	0.2093 (4)	0.6073 (4)	0.1158 (1)	0.048 (1)
C(18)	0.2914 (5)	0.7115 (4)	0.1120 (2)	0.059 (2)
C(19)	0.4124 (5)	0.7120 (5)	0.0879 (2)	0.068 (2)
C(20)	0.4553 (5)	0.6079 (5)	0.0663 (2)	0.063 (2)
C(21)	0.3779 (5)	0.5035 (5)	0.0687 (2)	0.058 (2)
C(22)	0.2573 (5)	0.5043 (4)	0.0929 (2)	0.058 (2)
C(23)	-0.1181 (4)	0.6976 (4)	0.1743 (1)	0.046 (2)
C(24)	-0.1327 (5)	0.8204 (4)	0.1644 (2)	0.063 (2)
C(25)	-0.2466 (6)	0.8903 (5)	0.1768 (2)	0.072 (2)
C(26)	-0.3499 (5)	0.8374 (6)	0.1997 (2)	0.079 (2)
C(27)	-0.3410 (5)	0.7169 (6)	0.2104 (2)	0.087 (2)
C(28)	-0.2268 (5)	0.6487 (4)	0.1981 (2)	0.070 (2)

[a] U_{eq} = one-third of the trace of the orthogonalized **U** matrix.

Scheme III

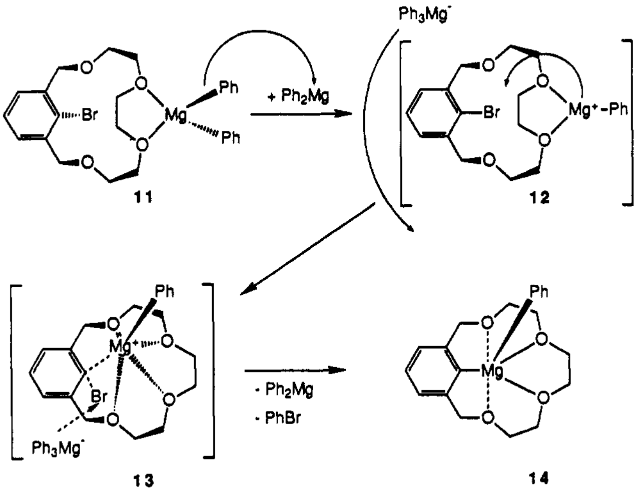

fastest reacting crown ether) in Scheme III.

We propose that between these reagents a 1:1 side-on complex **11** is formed which is analogous to **8**. Direct conversion of **11** to **14** is unlikely for the following reasons. In view of the high rigidity of the crown ether part of **11**, it is impossible for the phenyl anion to approach the bromine at the same time as the magnesium attacks the ipso carbon; dissociation of **11** to the cation **12** and a free phenyl anion in this medium (diethyl ether!) is not probable either. However, reaction of **11** with another diphenylmagnesium, derived from another **11** or from minute amounts of diethyl ether solvated diphenylmagnesium present in the solvation equilibria, could lead to the triphenylmagnesate salt of **12**. The PhMg$^+$ cation of **12** is not only more electrophilic but also much smaller than

Table IV. Final Coordinates and Equivalent Isotropic Thermal Parameters and Their Esd's in Parentheses for 10

atom	*x*	*y*	*z*	*U*(eq),[a] Å^2
		Molecule 1		
Zn(1)	-0.14153 (3)	0.34597 (2)	0.08931 (2)	0.0667 (2)
O(101)	0.1635 (2)	0.4058 (1)	0.1663 (1)	0.070 (1)
O(102)	-0.0311 (2)	0.4351 (1)	0.0877 (1)	0.063 (1)
O(103)	-0.1340 (2)	0.4191 (1)	0.1837 (1)	0.062 (1)
O(104)	-0.1182 (2)	0.3681 (1)	0.3203 (1)	0.072 (1)
O(105)	0.0676 (2)	0.3325 (2)	0.3830 (1)	0.086 (1)
C(101)	0.2025 (3)	0.3570 (2)	0.3150 (3)	0.067 (2)
C(102)	0.2181 (3)	0.3761 (2)	0.3832 (3)	0.068 (2)
C(103)	0.2961 (4)	0.4164 (3)	0.4128 (2)	0.080 (2)
C(104)	0.3555 (3)	0.4393 (3)	0.3740 (3)	0.091 (2)
C(105)	0.3388 (3)	0.4211 (3)	0.3051 (3)	0.085 (3)
C(106)	0.2618 (3)	0.3803 (2)	0.2750 (2)	0.068 (2)
C(107)	0.2396 (3)	0.3620 (2)	0.2005 (2)	0.086 (2)
C(108)	0.1232 (3)	0.3792 (2)	0.0998 (2)	0.075 (2)
C(109)	0.0512 (3)	0.4306 (2)	0.0627 (2)	0.076 (2)
C(110)	-0.0260 (3)	0.4881 (2)	0.1410 (2)	0.070 (2)
C(111)	-0.1174 (3)	0.4904 (2)	0.1595 (2)	0.069 (2)
C(112)	-0.2092 (3)	0.4169 (2)	0.2174 (2)	0.078 (2)
C(113)	-0.1961 (3)	0.3543 (2)	0.2660 (2)	0.079 (2)
C(114)	-0.0931 (3)	0.3068 (2)	0.3644 (2)	0.080 (2)
C(115)	-0.0064 (3)	0.3253 (2)	0.4155 (2)	0.084 (2)
C(116)	0.1512 (3)	0.3563 (3)	0.4254 (2)	0.097 (2)
C(117)	-0.0773 (3)	0.2580 (2)	0.1301 (2)	0.060 (2)
C(118)	-0.0845 (3)	0.1924 (3)	0.0942 (2)	0.082 (2)
C(119)	-0.0432 (4)	0.1290 (3)	0.1235 (3)	0.106 (3)
C(120)	0.0080 (4)	0.1285 (3)	0.1890 (3)	0.102 (3)
C(121)	0.0176 (3)	0.1921 (3)	0.2265 (3)	0.090 (2)
C(122)	-0.0229 (3)	0.2552 (2)	0.1965 (3)	0.075 (2)
C(123)	-0.2455 (3)	0.3847 (2)	0.0189 (2)	0.059 (2)
C(124)	-0.3259 (3)	0.3462 (2)	-0.0031 (2)	0.092 (2)
C(125)	-0.3982 (3)	0.3691 (3)	-0.0556 (3)	0.117 (3)
C(126)	-0.3923 (3)	0.4329 (3)	-0.0872 (2)	0.094 (2)
C(127)	-0.3150 (3)	0.4741 (3)	-0.0674 (2)	0.086 (2)
C(128)	-0.2430 (3)	0.4508 (3)	-0.0156 (2)	0.076 (2)
		Molecule 2		
Zn(2)	0.13359 (3)	0.67054 (2)	0.40337 (2)	0.0695 (2)
O(201)	-0.1631 (2)	0.5974 (1)	0.3138 (1)	0.067 (1)
O(202)	0.0320 (2)	0.5666 (1)	0.3855 (1)	0.072 (1)
O(203)	0.1501 (2)	0.6173 (1)	0.3070 (1)	0.069 (1)
O(204)	0.1370 (2)	0.6779 (2)	0.1777 (2)	0.100 (2)
O(205)	-0.0457 (2)	0.6804 (2)	0.0958 (2)	0.085 (1)
C(201)	-0.1912 (3)	0.6786 (2)	0.1788 (2)	0.062 (2)
C(202)	-0.2015 (3)	0.6760 (2)	0.1085 (3)	0.062 (2)
C(203)	-0.2759 (4)	0.6388 (3)	0.0699 (2)	0.082 (2)
C(204)	-0.3375 (3)	0.6044 (3)	0.1001 (3)	0.092 (3)
C(205)	-0.3277 (3)	0.6074 (2)	0.1700 (3)	0.081 (2)
C(206)	-0.2529 (3)	0.6441 (2)	0.2099 (2)	0.063 (2)
C(207)	-0.2359 (3)	0.6469 (2)	0.2865 (2)	0.090 (2)
C(208)	-0.1252 (3)	0.6081 (2)	0.3842 (2)	0.079 (2)
C(209)	-0.0502 (3)	0.5524 (2)	0.4079 (2)	0.078 (2)
C(210)	0.0369 (3)	0.5333 (2)	0.3232 (2)	0.082 (2)
C(211)	0.1294 (3)	0.5413 (2)	0.3098 (2)	0.078 (2)
C(212)	0.2289 (3)	0.6332 (2)	0.2802 (2)	0.087 (2)
C(213)	0.2105 (3)	0.6300 (3)	0.2046 (3)	0.101 (3)
C(214)	0.1161 (3)	0.6860 (3)	0.1072 (3)	0.100 (2)
C(215)	0.0271 (4)	0.7236 (2)	0.0832 (2)	0.094 (2)
C(216)	-0.1329 (3)	0.7150 (2)	0.0766 (2)	0.083 (2)
C(217)	0.0602 (3)	0.7566 (2)	0.3677 (2)	0.059 (2)
C(218)	0.0308 (3)	0.7695 (2)	0.2972 (2)	0.069 (2)
C(219)	-0.0161 (3)	0.8322 (3)	0.2713 (2)	0.078 (2)
C(220)	-0.0348 (3)	0.8854 (3)	0.3143 (3)	0.089 (3)
C(221)	-0.0079 (4)	0.8746 (3)	0.3835 (3)	0.101 (3)
C(222)	0.0382 (3)	0.8112 (3)	0.4089 (2)	0.081 (2)
C(223)	0.2348 (3)	0.6250 (2)	0.4723 (2)	0.064 (2)
C(224)	0.2176 (3)	0.5884 (3)	0.5286 (3)	0.088 (2)
C(225)	0.2874 (4)	0.5590 (3)	0.5792 (2)	0.094 (2)
C(226)	0.3773 (4)	0.5643 (2)	0.5739 (3)	0.086 (2)
C(227)	0.3971 (3)	0.5981 (2)	0.5184 (3)	0.081 (2)
C(228)	0.3264 (3)	0.6278 (2)	0.4686 (2)	0.072 (2)

[a] *U*(eq) = one-third of the trace of the orthogonalized **U** matrix.

Table V. Relevant Bond Distances (Å) and Angles (deg) for 8

Zn–O(2)	2.274 (6)	Zn–C(21)	1.959 (8)
Zn–O(3)	2.264 (6)	Zn–C(15)	1.962 (8)
O(2)–Zn–O(3)	71.6 (2)	O(3)–Zn–C(15)	108.1 (3)
O(2)–Zn–C(15)	107.9 (3)	O(3)–Zn–C(21)	101.6 (3)
O(2)–Zn–C(21)	107.1 (3)	C(15)–Zn–C(21)	139.6 (3)

Table VI. Relevant Bond Distances (Å) and Angles (deg) for 9

Zn–O(2)	2.239 (3)	Zn–C(23)	1.961 (4)
Zn–O(3)	2.328 (3)	Zn–C(17)	1.966 (4)
O(2)–Zn–O(3)	72.4 (1)	O(3)–Zn–C(17)	104.1 (1)
O(2)–Zn–O(17)	101.9 (2)	O(3)–Zn–C(23)	104.6 (1)
O(2)–Zn–C(23)	102.6 (1)	C(17)–Zn–C(23)	146.7 (2)

Table VII. Relevant Bond Distances (Å) and Angles (deg) for 10

Zn(1)–O(102)	2.310 (3)	Zn(2)–O(202)	2.393 (3)
Zn(1)–O(103)	2.300 (3)	Zn(2)–O(203)	2.228 (3)
Zn(1)–C(117)	1.947 (4)	Zn(2)–C(217)	1.949 (4)
Zn(1)–C(123)	1.964 (4)	Zn(2)–C(223)	1.973 (4)
O(102)–Zn(1)–O(103)	72.68 (9)	O(202)–Zn(2)–O(203)	73.4 (1)
O(102)–Zn(1)–C(117)	108.0 (1)	O(202)–Zn(2)–C(217)	107.9 (1)
O(102)–Zn(1)–C(123)	100.1 (1)	O(202)–Zn(2)–C(223)	96.8 (1)
O(103)–Zn(1)–C(117)	101.9 (1)	O(203)–Zn(2)–C(217)	101.3 (1)
O(103)–Zn(1)–C(123)	105.4 (1)	O(203)–Zn(2)–C(223)	102.1 (1)
C(117)–Zn(1)–C(123)	145.5 (2)	C(217)–Zn(2)–C(223)	149.9 (2)

Ph_2Mg; it can therefore move into the cavity to approach the aromatic xylyl 2-carbon (ipso) from above; in this process, it may be helped by additional coordination to the benzylic ether oxygens. Simultaneously, the nucleophilic part of the halogen–metal exchange proceeds by attack of the Ph_3Mg^- anion on bromine from underneath, as depicted in the transition state **13**, to yield **14** and bromobenzene. For the reactions of other crown ethers and organomagnesium compounds, an analogous course of events can be envisaged. Note that the coordination mode of **5** (Scheme II) has been modeled after the experimentally observed structures of **9** and **10**.

The inability of diphenylzinc to metalate the xylyl 2-position can be explained by the relatively low polarity of the zinc–carbon bond, which was also assumed to be the reason for the nonoccurrence of rotaxane formation with **4** (vide supra).

Experimental Section

Reactions and crystallizations using diphenylzinc were carried out in fully sealed glassware, using high-vacuum techniques. Dry solvents were prepared by distillation from liquid Na/K alloy in sealed glassware, after predrying on NaOH. Yields of the organozinc compounds were determined by hydrolysis followed by titration with HCl for base and EDTA for Zn^{2+}. The crown ethers **1**–**4**[1,2,21] were synthesized in analogy to literature procedures[17] from the appropriate oligo(ethylene glycol) and 1,3-bis(bromomethyl)benzene (**2**, **3**) or 2-bromo-1,3-bis(bromomethyl)benzene (**1**, **4**), using potassium hydride in THF. Diphenylmercury (Merck) and zinc metal (Ventron, high-purity grade) were commercially available. ^{1}H NMR spectra were measured on a Bruker WH 90 or a Bruker WM 250. GC–MS analyses were performed on a HP 5800 GC/5970 MS combination, operating at 70 eV and equipped with a Chrompack CP Sil 19CB 51-m/0.21-mm column.

Diphenylzinc. Diphenylmercury (7.1 g, 20 mmol) was stirred with zinc (13 g, 200 mmol) for 2 weeks in diethyl ether (200 mL). The clear, light-brown solution was decanted from the zinc amalgam. An aliquot of this solution was titrated to check complete conversion of the organomercury starting material. The expected concentrations of base and Zn^{2+} were found in a ratio of 2.01:1. The solution was divided into ampules containing 1 mmol of Ph_2Zn in 10 mL of Et_2O.

General Procedure for the Complexation of Ph_2Zn with a Crown Ether (1–4). In a fully sealed glass assembly connected to a high vacuum line, 1.0 mmol of the pure crown ether was high-vacuum pumped (degassed) to $<5 \times 10^{-6}$ mbar. After sealing off the apparatus, the crown ether was dissolved in 1–2 mL of diethyl ether. This solution was stirred with diphenylzinc (1.0 mmol, in 10 mL of Et_2O) to yield a clear solution. Upon slow concentration and/or cooling, colorless crystals were formed, which were separated from the solvent by decantation and divided into several samples. One of these samples was transferred into a dry nitrogen glovebox (Braun, Garching, Germany) and high-quality single crystals were transferred to Lindemann capillaries for crystal structure determination. The remaining crystals were used for ^{1}H NMR characterization, titration (Zn^{2+} and base), or quench reactions (H_2O, D_2O) to check their identity. For a ^{1}H NMR analysis, the crystals were pumped to high-vacuum pressure ($<10^{-5}$ mbar) to remove the noncoordinating solvent, before the deuterated solvent was added. Essential for successful reactions is the high purity of the crown ethers **1**–**4**; this can be archieved by crystallization from Et_2O/*n*-pentane at −20 °C (**2**, **3**, and **4**: mp 44, 42, and 43 °C, respectively) or by high-vacuum distillation [**1**, a liquid at room temperature, bp 120 °C (5×10^{-6} mbar)].

2-Bromo-1,3-xylyl 15-Crown-4–Diphenylzinc (8). The ^{1}H NMR spectrum of the crystalline solid revealed the formation of a solvent-free 1:1 complex (250 MHz, toluene-d_8; ref $C_6D_5CD_2H$ at δ 2.32 ppm): δ 3.16–3.24 (m, 2 H, CH_2), 3.40–3.49 (m, 2 H, CH_2), 3.46 (s, 4 H, C_2H_4), 3.50–3.58 (m, 2 H, CH_2), 3.73–3.83 (m, 2 H, CH_2), 4.59 (m (AB), $\Delta\delta = 1.26$ ppm, $^2J = 13$ Hz, 4 H, xylyl CH_2), 7.03 (d, $^3J = 7$ Hz, 2 H, xylyl H(4,6)), 7.20 (t, $^3J = 7$ Hz, 1 H, xylyl H(5)), 7.48–7.53 (m, 6 H, phenyl H(3,4,5)), 7.61–7.65 (m, 4 H, phenyl H(2,6)). To quantify the effects of complexation on the crown ether shifts, a reference spectrum of pure **2** was measured under the same conditions: δ 3.14–3.24 (m, 4 H, C_2H_4), 3.28–3.35 (m, 4 H, C_2H_4), 3.43–3.65 (m, 8 H, C_2H_4), 4.78 (m(AB), $\Delta\delta = 0.914$ ppm, $^2J = 13$ Hz, 4 H, xylyl CH_2), 7.12–7.23 (m, 3 H, xylyl H). The remaining crystals were quenched by adding some aqueous HCl (1 N). The organic material was isolated by repeated extraction with dichloromethane. The organic phase was dried ($MgSO_4$), filtered, and evaporated to dryness. The residual colorless oil was found to be pure **2** (^{1}H NMR, 90 MHz, $CDCl_3$); **1** was not detected.

Behavior of 8 at Elevated Temperatures. A 1-mmol sample of **8** was suspended in toluene (10 mL) and heated for 6 h at 100 °C. During this period, a clear colorless solution was formed. After cooling to room temperature, the reaction mixture was quenched with D_2O (0.5 mL). Aqueous HCl (1 N) was added and the toluene layer separated, followed by repeated extraction with CH_2Cl_2. The combined organic fractions were dried ($MgSO_4$), filtered, and evaporated to dryness. The residue (0.31 g of a colorless solid, 94% yield) was characterized by ^{1}H NMR (90 MHz, $CDCl_3$) as pure **2**; no **1** was detected.

2-Bromo-1,3-xylyl 18-Crown-5–Diphenylzinc (9). Crystals were prepared in almost quantitative yield by the method described above. Once formed, the complex had a low solubility in diethyl ether. A ^{1}H NMR analysis revealed the formation of a solvent-free 1:1 complex (250 MHz, C_6D_6; ref C_6D_5H at δ 7.17 ppm): δ 3.17 (s, 8 H, CH_2), 3.38–3.41 and 3.54–3.56 (m (A_2B_2), 8 H, CH_2), 4.38 (s, 4 H, xylyl CH_2), 6.99–7.02 (m, 3 H, xylyl H), 7.39–7.43 (m, 6 H, phenyl H(3,4,5)), 7.77–7.80 (m, 4 H, phenyl H(2,6)).

Behavior of 9 at Elevated Temperature. A sample of **9** (about 0.6 mmol) was dissolved in toluene (10 mL) and heated for 6 h at 100 °C. After cooling to room temperature, the sample was quenched with D_2O (excess, 0.5 mL). Aqueous HCl (1 N) was added and the toluene layer separated, followed by several extractions with CH_2Cl_2. The combined organic phases were dried ($MgSO_4$), filtered, and evaporated to dryness. The residue (colorless solid, 0.2 g) was characterized by ^{1}H NMR ($CDCl_3$, 90 MHz) as pure **3**; **4** was not detectable.

1,3-Xylyl 18-Crown-5–Diphenylzinc (10). Crystals were prepared as described above. As only a small amount of solid was formed (24% yield), the mother liquor was titrated (base, 1.52 mmol; Zn^{2+}, 0.76 mmol). Part of the crystalline material was dissolved in toluene-d_8 and characterized as the solvent-free 1:1

---

(21) Markies, P. R.; Nomoto, T.; Akkerman, O. S.; Bickelhaupt, F.; Smeets, W. J. J.; Spek, A. L. *J. Am. Chem. Soc.* **1988**, *110*, 4284.

Table VIII. Analysis of the Ph_2Zn Coordination Geometry in Various Complexes

	8	9	10a	10b	Ph_2Zn·glyme[a]
		Bond Angles, deg			
C–Zn–C	139.6 (3)	146.7 (2)	145.5 (2)	149.9 (2)	146.6 (2)
O–Zn–O	71.6 (2)	72.4 (1)	72.68 (9)	73.4 (1)	72.2 (1)
C–Zn–O	101.6 (3)	101.9 (2)	100.1 (1)	96.8 (1)	102.4 (1)
	107.1 (3)	102.6 (1)	101.9 (1)	101.3 (1)	103.1 (2)
	107.9 (3)	104.1 (1)	105.4 (1)	102.1 (1)	103.3 (2)
	108.1 (3)	104.6 (1)	108.0 (1)	107.9 (1)	104.8 (2)
		Bond Distances, Å			
Zn–O	2.264 (6)	2.239 (3)	2.300 (3)	2.228 (3)	2.259 (4)
	2.274 (6)	2.328 (3)	2.310 (3)	2.393 (3)	2.287 (4)
Zn–C	1.959 (8)	1.961 (4)	1.947 (4)	1.949 (4)	1.958 (5)
	1.962 (8)	1.966 (4)	1.964 (4)	1.973 (4)	1.969 (5)

[a] Markies, P. R.; Schat, G.; Akkerman, O. S.; Bickelhaupt, F.; Spek, A. L. *J. Organomet. Chem.*, in press.

complex **10** by ^1H NMR spectroscopy (250 MHz; ref $C_6D_5CD_2H$ at δ 2.32 ppm): δ 3.46–3.50 (m (A_2 part of A_2B_2 system), 4 H, CH_2), 3.54–3.62 (m (B_2 part of A_2B_2 system, A'_2 part of $A'_2B'_2$ system), 8 H, CH_2), 3.66–3.72 (m (B'_2 part of $A'_2B'_2$ system), 4 H, CH_2), 4.46 (s, 4 H, xylyl CH_2), 7.07 (d, ^3J = 7 Hz, 2 H, xylyl H(4,6)), 7.29 (t, ^3J = 7 Hz, 1 H, xylyl H(5)), 7.53 (tt, ^3J = 7 Hz, ^4J = 2 Hz, 2 H, phenyl H(4)), 7.63 (ddm, ^3J = 8 Hz, ^3J = 7 Hz, 4 H, phenyl H(3,5)), 8.16 (dd, ^3J = 8 Hz, ^4J = 2 Hz, 4 H, phenyl H(2,6)), 8.22–8.23 (m, 1 H, xylyl H(2)). To determine the effects of complexation on the crown ether shifts, a spectrum of pure **4** was measured under the same conditions: δ 3.66–3.67 (m, A_2B_2, 8 H, CH_2), 3.67–3.71 and 3.73–3.77 (m, $A'_2B'_2$, 8 H, CH_2), 4.68 (s, 4 H, xylyl CH_2), 7.21 (d, ^3J = 7 Hz, 2 H, xylyl H(4,6)), 7.35 (t, ^3J = 7 Hz, xylyl H(5)), 8.16 (m, 1 H, xylyl H(2)).

Reaction between 1,3-Xylyl 15-Crown-4 (1) and Diphenylzinc. From this reaction, no crystalline complex was obtained. Upon mixing the components in a 1:1 ratio (1 mmol of each in 10 mL of Et_2O) and removing the solvent, a colorless oil containing some precipitate (Ph_2Zn?) was formed. To check whether a metalation reaction could be induced, this mixture was dissolved in toluene (10 mL); it gave a clear solution and was heated for 6 h to 100 °C. After cooling to room temperature, the solution was quenched with D_2O (about 0.5 mL). Aqueous HCl (1 N) was added, the toluene layer separated, and the organic material collected by repeated extraction with dichloromethane. The combined organic layers were dried ($MgSO_4$), filtered, and evaporated to dryness. The remaining residue (colorless oil, 0.22 g, 87% yield) was characterized by ^1H NMR spectroscopy ($CDCl_3$, 90 MHz) and GC–MS as pure **1**; deuterium incorporation was not detected.

Structure Determination and Refinement of 8–10. Crystal data and numerical details of the structure determinations are given in Table I. The crystals were mounted under nitrogen in Lindemann glass capillaries and transferred to an Enraf-Nonius CAD4F diffractometer for data collection. Unit cell parameters were determined from a least-squares treatment of the SET4 setting angles of 25 reflections and were checked for the presence of higher lattice symmetry.[22] All data were collected with an $\omega/2\theta$ scan mode. Data were corrected for Lp and for the observed linear decay of the reference reflections. Absorption correction was applied for **8**, using the DIFABS method;[23] redundant data were merged into an unique data set. Standard deviations as obtained by counting statistics were increased according to an analysis of the excess variance of the reference reflections: $\sigma^2(I) = \sigma^2_{cs}(I) + (PI)^2$ with P = 0.033, 0.037, and 0.011 for **8**, **9**, and **10**, respectively.[24] The structures were solved with either standard Patterson methods (**8**, **10**) or direct methods (**9**) (SHELXS86)[25] and subsequent difference Fourier syntheses. Refinement on F was carried out by full-matrix least-squares techniques. Relatively large thermal motion components for C(10) and C(11) in **8** probably indicate conformational disorder. No disorder model was attempted in view of the limited number of observed data. H atoms were introduced on calculated positions (C–H = 0.98 Å) and included in the refinement riding on their carrier atoms. All non-hydrogen atoms were refined with anisotropic thermal parameters; H atoms were refined with one (**8**, **9**) or two (**10**) common isotropic thermal parameters. F_c values of **9** were corrected for secondary extinction by refinement of an empiric isotropic parameter X (=1.07 (8) × 10^{-7}, $F_c' = F_c(1 - XF^2/\sin\theta)$). Weights were introduced in the final refinement cycles.

Final atomic coordinates and equivalent isotropic thermal parameters are listed in Tables II–IV; geometrical data are given in Tables V–VII. Neutral atom scattering factors were taken from Cromer and Mann and corrected for anomalous dispersion.[26,27] All calculations were performed with SHELX76[28] and the EUCLID package (geometrical calculations and illustrations)[29] on a MicroVAX cluster.

Acknowledgment. X-ray data were collected by A. J. M. Duisenberg. This work was supported in part (P.R.M., W.J.J.S., A.L.S.) by the Netherlands Foundation for Chemical Research (SON) with financial aid from the Netherlands Organization for Scientific Research (NWO).

Supplementary Material Available: Tables of anisotropic thermal parameters, all H atom parameters, bond lengths, bond angles, and selected torsion angles and thermal ellipsoid plots for 8–10 (21 pages); listings of observed and calculated structure factor amplitudes for 8–10 (124 pages). Ordering information is given on any current masthead page.

---

(22) Spek, A. L. *J. Appl. Crystallogr.* **1988**, *21*, 578.

(23) Walker, N., Stuart, D. *Acta Crystallogr. A* **1983**, *39*, 158.

(24) McCandlish, L. E., Stout, G. H., Andrews, L. C. *Acta Crystallogr. A* **1975**, *31*, 245.

(25) Sheldrick, G. M. SHELXS86, Program for crystal structure determination, University of Göttingen, Federal Republic of Germany, 1986.

(26) Cromer, D. T.; Mann, J. B. *Acta Crystallogr. A* **1968**, *24*, 321.

(27) Cromer, D. T.; Liberman, D. *J. Chem. Phys.* **1970**, *53*, 1891.

(28) Sheldrick, G. M. SHELX76, Crystal structure analysis package, University of Cambridge, England, 1976.

(29) Spek, A. L. The EUCLID Package. In *Computational Crystallography*; Sayre, D., Ed.; Clarendon Press: Oxford, 1982; p 528.